The origin of size-selective gas transport through Polymers of Intrinsic Microporosity.

Received 00th January 20xx,
Accepted 00th January 20xx

DOI: 10.1039/x0xx00000x

Alessio Fuoco[a]*, Carmen Rizzuto[a†], Elena Tocci[a], Marcello Monteleone[a], Elisa Esposito[a], Peter M. Budd[b], Mariolino Carta[c], Bibiana Comesaña-Gándara[d], Neil B. McKeown[d], Johannes C. Jansen[a]

An analysis of the diffusivity–of light gases through Polymers of Intrinsic Microporosity (PIMs) shows that smaller H_2 and He gas molecules have a transport mechanism that is similar to that of porous materials, whereas larger gas molecules, CH_4, N_2, O_2 and CO_2, show activated transport similar to that of conventional dense polymers. A typical and *defining* feature of PIMs, which differentiate their properties from other high free volume polymers, glassy polymers and rubbers, is the change in slope of the plot of the diffusion coefficient as a function of the gas diameter, with a stronger size-selective trend for the larger gas molecules than for He and H_2. Deviation from this trend is observed for a polymer-gas combination with strong mutual affinity (i.e. an amine modified PIM with CO_2). Molecular modelling shows that size selectivity in PIMs originates from the presence of bottlenecks between the individual free volume elements. For the latest generation of highly rigid PIMs, ageing studies show that diffusivity is differentially reduced for larger gas molecules, thus further enhancing their size-selectivity.

Membrane technology can reduce humanity's environmental footprint by minimizing the use of raw materials and reducing energy consumption, in some cases by an order of magnitude with respect to traditional separation processes.[1–3] In gas separation, polymeric membranes are already used in several industrial processes, such as N_2 generation, O_2 enrichment of air, hydrogen recovery, natural gas upgrading, and are strongly emerging as the technology of choice for biogas purification.[4] Membranes are also showing potential for use in pre- and post-combustion CO_2 capture.[5] However, a more rapid deployment of membrane technology is limited by the lack of suitable materials with appropriate gas transport properties, and by the uncertainties about their robustness under different operating conditions and long-term stability. Despite many hundreds of new polymers being assessed, only about a dozen are used in commercial membranes – mainly cellulose acetates, polyimides, polysulfones and polyethersulfones.[6] These polymers offer high selectivity but low permeability, which necessitates the use of large membrane areas to compensate for low permeance.[5] In order to be competitive with other conventional processes, especially for large-volume applications like CO_2 capture from flue gas or natural gas processing, polymers with higher permeability are required to reduce membrane costs and the system footprint.[6] Inspired by the growing awareness of climate change by greenhouse gas emissions, there has been an increasing effort to make novel membrane materials with high permeability. Examples of highly permeable polymers include poly[1-(trimethylsilyl)-1-propyne] (PTMSP), reported for the first time in 1983 and for many years the most permeable polymer known,[7] other polyacetylenes,[8] glassy perfluoropolymers,[9–11] and thermally rearranged (TR) polymers[12]. Of particular importance, the ladder-like Polymers of Intrinsic Microporosity (PIMs),[13,14] introduced in 2004 by Budd, McKeown *et al.,*[15] are highly permeable due to the inefficient packing of rigid and contorted polymer chains. However, despite systematic synthetic development of the PIMs concept, there is insufficient mechanistic understanding of their relatively high selectivity for one gas over another. This study seeks to fill that gap by a detailed analysis of their gas transport properties.

Since 1940, the permeability (P_a) of a gas *a* through a dense polymer has been described by the solution-diffusion model.[16,17] P_a is given by the product of only two parameters: diffusivity (D_a) and solubility (S_a), i.e. $P_a=D_a\times S_a$. The ideal selectivity (α) for a gas pair *x* and *y* is defined by the ratio of the permeability of the two species and can be split into the individual terms for diffusivity and solubility:

$$\alpha_{ab}=P_a/P_b=(D_a/D_b)\times(S_a/S_b) \quad (1)$$

The permeability of the most permeable gas and the ideal selectivity are thus the indicators with which the possible gas separation performance of novel materials is evaluated. In 1991, Robeson recognized that for polymers there is a trade-off between the ideal selectivity of a gas pair and permeability.[18] This trade-off results in a series of empirical upper bounds drawn in Robeson's plot of $\log\alpha_{ab}$ versus $\log P_a$ for a number of gas pairs of industrial interest. Subsequently, these upper bounds have been revised to higher values of permeability and selectivity.[18–21] In a theoretical analysis, Freeman suggests that high free volume and very stiff polymer chains are necessary to develop high performing membranes, indicating that the selectivity for diffusivity (D_a/D_b) is the key factor to surpass the existing Robeson upper bounds.[22] These suggestions have been incorporated into the design criteria for PIMs, the performance of which have caused the revisions of the Robeson upper bounds.[19–21]

Here we investigate the gas transport mechanism in PIMs and compare them to other polymers (both glass and rubber)

[a.] *Institute on Membrane Technology (ITM-CNR), Via P. Bucci 17/C, 87036 Rende (CS), Italy.*
[b.] *Department of Chemistry, The University of Manchester, Manchester M13 9PL, U.K.*
[c.] *Department of Chemistry, College of Science, Singleton Park, Swansea University, Swansea, SA2 8PP, U.K.*
[d.] *EaSTChem, School of Chemistry, University of Edinburgh, David Brewster Road, Edinburgh EH9 3FJ, U.K.*
† Present Address Department of Physics, University of Calabria, Via P. Bucci Cubo 31/C, Rende, CS, Italy

Electronic Supplementary Information (ESI) available: Experimental gas separation method, Molecular Modelling Details, Molecular structure of the polymers, additional figures, tables with gas diffusion coefficients and fitting parameters. See DOI: 10.1039/x0xx00000x

and porous materials by assessing in detail the diffusivity of light gases. The effect of physical ageing, and the anomalous behavior for a PIM with a specific affinity for CO_2 are also discussed. With the aid of molecular modelling we illustrate the origin of the exceptional performance of PIMs.

Previously, we correlated the gas diffusion coefficient of PIMs[23–27] and TR polymers[28] with gas diameter. Previous studies have also focused on the correlation of the diffusion coefficient of gases and their molecular properties.[29] The common feature of these analyses is that the diffusivity exponentially decreases with the square of the gas diameter, although slightly different effective diameters were defined in these studies in order to obtain the best correlation. Table 1 lists the effective diameters used by Dal-Cin,[30] Robeson,[31] and Teplyakov and Meares (T-M),[32] in comparison with the Lennard-Jones (L-J) diameter and the kinetic diameter[33] for the gases used in the present study. T-M use the correlation between the diffusion coefficients of spherical noble gases to calculate those of all other gases, whereas others use methane as the reference point.[31] This results in an overall smaller effective diameter (d_α) calculated by T-M, but with a better correlation with the diffusivity (D_α) for the gases of interest in this study. The correlation with the square of the gas diameter (d_α^2) is due to the fact that the resistance to transport depends on the cross-sectional area of the diffusing molecule, which is related to the size of the void that must be created in the polymer matrix for the molecule to be able to move.[32] The T-M diameters give a systematically better correlation as compared to the other diameters (Table SI 1) and, therefore, were used in this work. Indeed, good to excellent correlation was found for all gases for D_α *versus* d_α^2 for the rubbery polymer Pebax®2533, a glassy high free volume polymer Hyflon®AD60x, and a conventional glassy polymer PEEK-WC (structures of all polymers for which data are reported are given in Fig. SI 1).

Although Robeson *et al.*[34] also suggested a linear correlation for gas diffusion in PIMs and TR polymers, we observe that for a typical PIM (e.g., PIM-MP-TB) there is a linear trend for the larger O_2, CO_2, N_2 and CH_4, and a different linear trend for the smaller gases H_2 and He (Figure 1), and this seems to be a typical feature of PIMs. To the best of our knowledge, PIMs are the only class of *soluble* (i.e. membrane-forming) polymer to show this marked difference in correlation for H_2 and He.

Table 1. Gas diameters (Å) from the Lennard-Jones theory (L-J), kinetic diameters determined from their motion in porous media (Breck), and the effective diameters based on semi-empirical correlations of gas transport in polymers proposed by different authors.

Gas	L-J[35]	Breck[33]	Dal-Cin[30]	Robeson[31]	T-M[32]
N_2	3.71	3.64	3.59	3.57	3.04
O_2	3.46	3.46	3.37	3.35	2.89
CO_2	4.07	3.30	3.43	3.33	3.02
CH_4	3.82	3.80	3.88	3.82	3.18
H_2	2.93	2.89	2.85	2.88	2.14
He	2.56	2.60	2.56	2.64	1.78

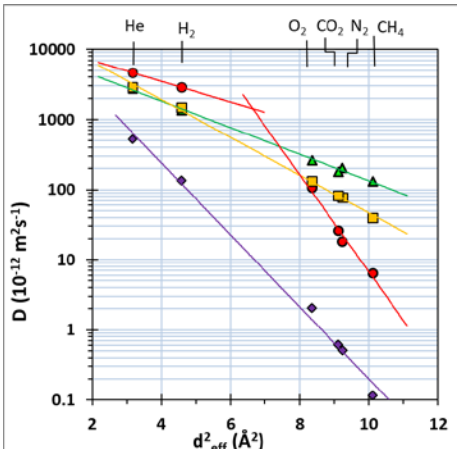

Figure 1. Correlation of the diffusion coefficient with the square of the Teplyakov-Meares gas diameter for Pebax®2533[36] (△), Hyflon®AD60x[37] (□), PEEK-WC [This work,38] (◆) and PIM-MP-TB[25] (●). The numerical data and the related fitting parameters are reported in Table SI 1 and Table SI 2.

The determination of the diffusivity of H_2 and He within a PIM is reliant on the extremely fast response of the time-lag permeation equipment (less than 0.1 s), which is fast enough to measure even very short time-lags.[39] The suitability of this time-lag methodology is confirmed by analogous measurements using the ultrapermeable polymer PTMSP that also has very high permeability coefficients for H_2 and He. For PTMSP the correlation of D_α *versus* d_α^2 is linear for all gases including He and H_2 (Figure 2), which is in contrast to all PIMs studied to date, including the recently reported ultrapermeable PIMs.[21,24] The origin of the higher selectivity for PIMs as compared to PTMSP lies in their greater size-selectivity, which is correlated to the much steeper slope of D_x *versus* d_x^2 for the bulkier gases (O_2, CO_2, N_2 and CH_4). Interestingly, for three samples with similar oxygen permeability, i.e. PTMSP, PIM-TMN-SBI and PIM-TMN-Trip (as an aged film), the solubility selectivity (S_{O_2}/S_{N_2}) is effectively constant (1.05-1.30). For PTMSP, the polymer with the gentlest slope for D_x *versus* d_x^2, its permeability/selectivity data is far below the original 1991 Robeson O_2/N_2 upper bound, whereas for PIM-TMN-Trip, the polymer with the steepest slope, its data are close to the proposed 2015 O_2/N_2 upper bound (Fig. 2a and b). For PIM-TMN-Trip the sharp decrease of D_x as a function of the penetrant dimension when a defined threshold is reached is similar to that observed for classic inorganic microporous materials such as zeolites like SAPO-34 that possess well-defined pores.[40] It suggests that the free volume elements in PIMs are interconnected by windows with an intermediate size between the smaller and the bulkier gases as illustrated by modelling of chain packing (see below).

Figure 3 shows the optimized chain-packing models of rubbery Pebax®2533 and glassy PEEK-WC, Hyflon®AD60x, and

PIM-MP-TB, showing free volume elements (FVEs) that are accessible to H_2, N_2, and CH_4, respectively. The simulations were performed with the Materials Studio software package (Accelrys) [41] using the COMPASS[42] force field. The rubbery Pebax®2533, which owes its permeability mainly to the rapid thermal motion of its chains due to its sub-ambient glass transition temperature, has virtually no *permanent* accessible fractional free volume. For the glassy polymers, small molecules such as H_2 can access more free volume than the bulkier N_2 and CH_4. In spite of its relatively high free volume, the glassy perfluoropolymer Hyflon® AD60x has few interconnected FVEs. In contrast, PIM-MP-TB is highly interconnected for H_2, and less so for N_2 and CH_4. This interconnectivity is responsible for the high mobility of the penetrants in PIMs, while the bottlenecks between the free volume elements, which may be accessible for one species but not for a slightly larger one (inserts in Figure 3), determine their strong size selectivity. Even if the molecule experiences a large amount of accessible free volume, its diffusion is determined by the energy barrier that must be overcome in order to open a motion-enabled zone between micropores,[43] as demonstrated by the thermal dependence of gas permeability of PIM-BTrip and PIM-TMN-Trip.[44] Thus, extreme chain rigidity leads to a sharp decrease of D_x for bulkier gas molecules even in the presence of highly accessible fractional free volume, as shown in Figure SI 1. With decreasing temperature, the different D_x *versus* d_x^2 correlation slopes for small and larger gas molecules remain, and the size-selectivity increases further (Figure SI 2), making PIMs potentially interesting materials for sub-ambient gas separations.

Interestingly, freshly solution cast films of substituted hexaphenylbenzene-based PIMs[45] (Figure SI 3) and thioamide-PIM-1[23] show a near linear correlation for all gases, including H_2 and He. In this state, residual solvent molecules occupy free volume elements[46] and the diffusion occurs as in traditional, non-microporous polymers. Typical PIM-like behaviour is induced by methanol treatment of the film to remove the residual solvent.

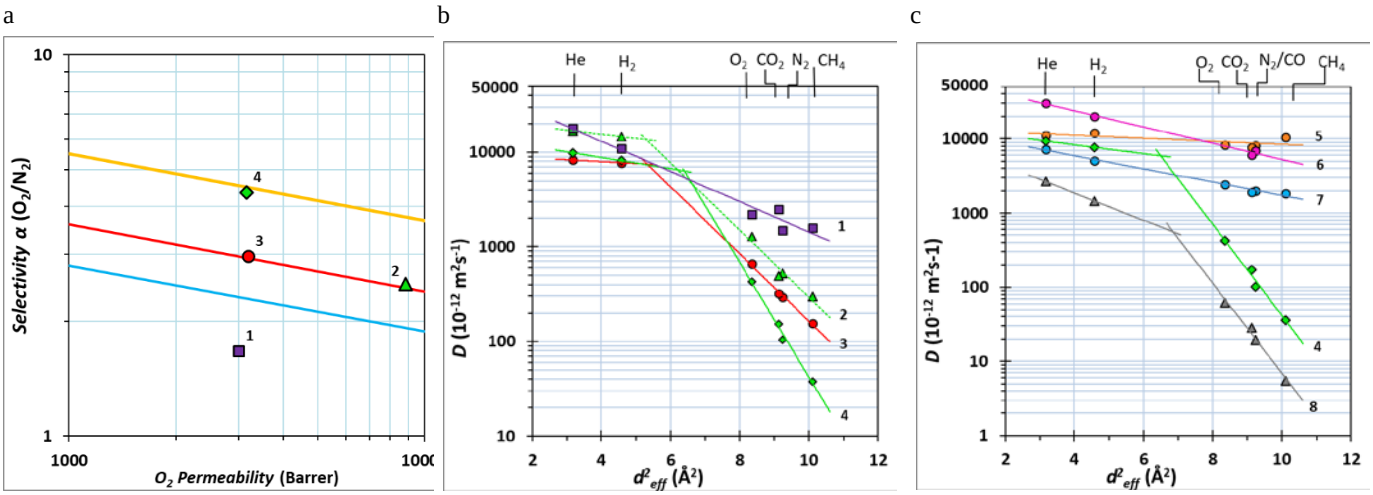

Figure 2. (**a**) Position of data in the Robeson diagram for the O_2/N_2 gas pair relative to the 1991 (blue), 2008 (red) and 2015 (yellow) upper bounds for the polymers PTMSP[47] (**1**); PIM-TMN-Trip after MeOH treatment[24]; (**2**) PIM-TMN-SBI after MeOH treatment[24] (**3**); PIM-TMN-Trip after thermal treatment and PIM-TMN-Trip after 1 year of ageing[24] (**4**); (**b**) D_a *versus* d_a^2 correlation for the same polymers as in (a); (**c**) D_a *versus* d_a^2 correlation for PIM-TMN-Trip after MeOH treatment[24] (**4**), Buckypaper[48] (**5**), large-pore zeolites, MFI[49] (**6**), water[50–52] (**7**), and the Thermally rearranged T-PIM-PBO-1[28] after ethanol treatment (**8**). The numerical data and the related fitting parameters are reported in Table SI 1 and Table SI 2.

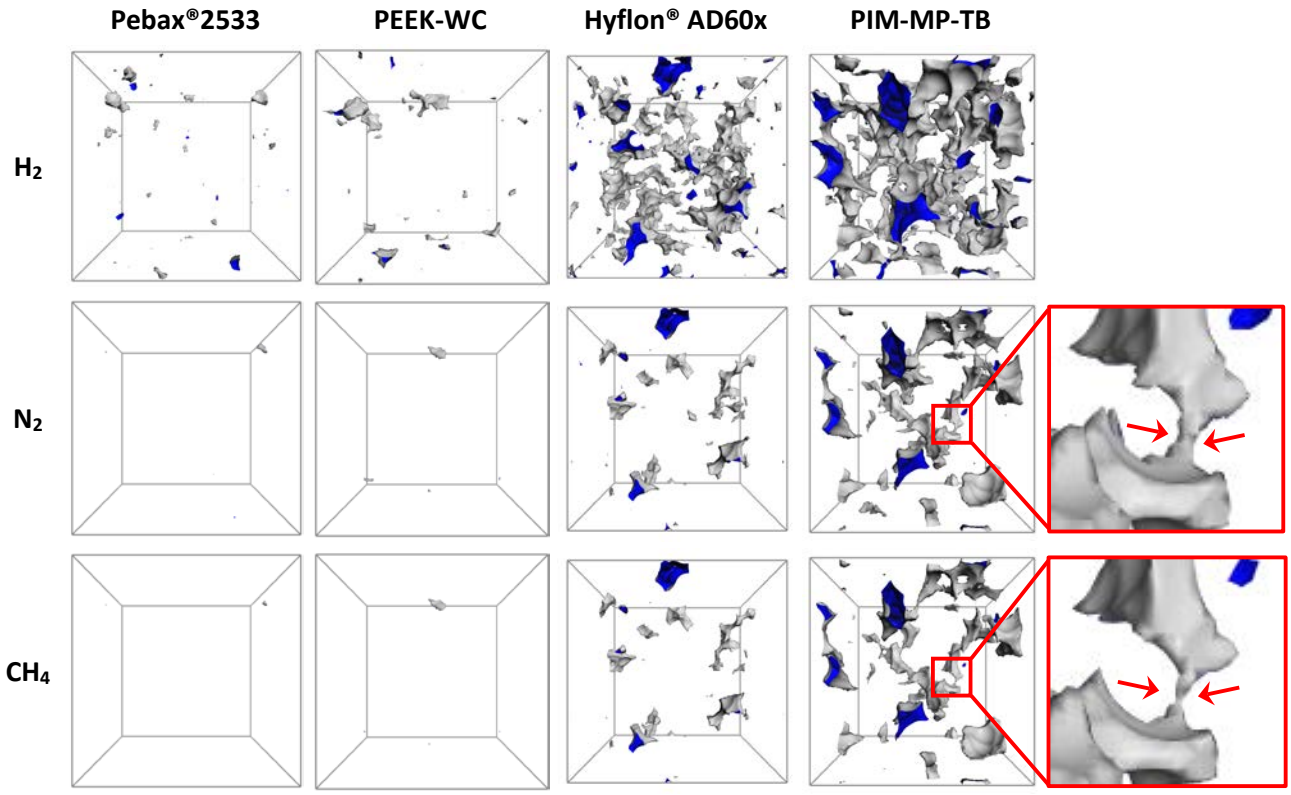

Figure 3. Molecular models showing the accessible fractional free volume for H_2, N_2 and CH_4 in Pebax®2533,[53] PEEK-WC,[54] Hyflon® AD60x[55] and PIM-MP-TB.[25] The inserts are zoom-ins of the connection between two free volume elements for N_2 and CH_4. Grey shading indicates the free volume elements seen from the outside, facing the polymer; blue shading indicates the inside of the free volume elements. The computational details are given in the supporting information and correlated references.

On ageing of PIM films, the size-selectivity also increases (Figure 4)[21,56] and the extent to which this occurs is fundamentally different for gas pairs involving He or H_2, for which the accessible free volume remains more interconnected and, hence, the reduction in diffusivity is modulated. To illustrate this behavior for PIM-BTrip, on aging, its data points move further away from the D_{He}/D_{N_2} correlation for glassy polymers defined by Robeson *et al.* (Figure 4).[57] In contrast, on aging, the data points for PIM-BTrip remain parallel to the correlation of Robeson *et al.* for D_{CO_2}/D_{N_2}. This suggests that changes in the pore size distribution and the tightening of the interconnectivity, due to rearrangement of the free volume elements during the ageing process, have a stronger impact on the diffusion of bulkier gases, while high interconnectivity is still maintained for lighter gases.

The correlation of diffusion coefficient with molecular size is a powerful tool to investigate anomalous transport phenomena. For example, conversion of the nitrile groups of PIM-1 into amino groups (to give amine-PIM-1) was anticipated to increase the affinity of the polymer towards CO_2 and, therefore, increase its selectivity over N_2 or CH_4, but surprisingly gave the opposite result.[56,58] Figure 5 shows that the diffusion coefficient of CO_2 within amine-PIM-1 is dramatically reduced by this modification as compared to that within unmodified PIM-1. This results in lower CO_2 permeability because the loss in diffusivity is not compensated by a sufficient increase in CO_2 solubility.

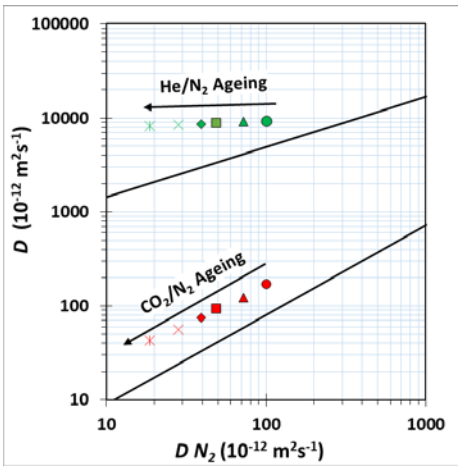

Figure 4. Relative changes of the diffusion coefficients of He /N_2 and CO_2/N_2 in PIM-BTrip upon ageing. Experimental data from Comesana-Gandara *et al.*[21]. The solid line represents the fitted average of glassy polymers reported by Robeson *et al.*[57] The

numerical data and the related fitting parameters are reported in Table SI 1 and Table SI 2.

For all other gases the two polymers behave similarly. Hence, it can be concluded that the enhanced CO_2-philic properties of amine-PIM-1 effectively results in a partial immobilization of CO_2 and a reduction in diffusion coefficient, which is clearly demonstrated by its strong deviation from the normal D_x *versus* d_x^2 trend. Plotting of the diffusion coefficient as a function of the gas diameter in this case confirms the presence of specific non-covalent interaction,[56] and can thus be used to trace anomalous transport properties.

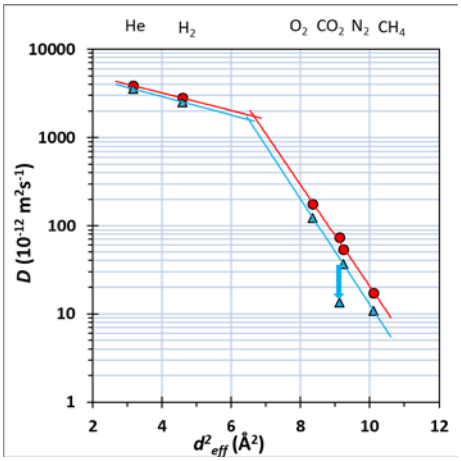

Figure 5. Correlation of the diffusivity and effective gas diameter in MeOH treated PIM-1 (●) and amine-PIM-1 (▲) evidencing the anomalous diffusion of CO_2. Data from Satilmis *et al.*[56] The numerical data and the related fitting parameters are reported in Table SI 1 and Table SI 2.

Conclusions

This analysis of the correlation of the diffusion coefficient and the effective diameter of gases for PIMs provides insight into the understanding of all gas separations, including those of commercial importance such as CO_2/CH_4, O_2/N_2, and H_2/N_2. It reveals that small molecules such as He and H_2 experience the fractional free volume as interconnected. Small gas molecules therefore permeate predominantly via the pore diffusion mechanism rather than the activated solution-diffusion mechanism, leading to a non-linearity that appears to be general and, together with solution processability, a *defining* feature of PIMs.[23–27] As a result, ageing of PIMs affects small molecules much less than large gas molecules. In addition, such correlations provide an excellent probe for the identification of anomalous phenomena in the case of strong polymer-penetrant interactions.

Conflicts of interest

The authors declare no competing financial interest.

Acknowledgements

The work leading to these results has received funding from the European Union's Seventh Framework Program (FP7/2007-2013) under grant agreements n° 608490, project M^4CO_2 and from the EPSRC (UK) grant numbers EP/M01486X/1, EP/R000468/1 and EP/K008102/2

References

1 E. Drioli and E. Fontananova, *Annu. Rev. Chem. Biomol. Eng.*, 2012, **3**, 395–420.
2 D. F. Sanders, Z. P. Smith, R. Guo, L. M. Robeson, J. E. McGrath, D. R. Paul and B. D. Freeman, *Polym. (United Kingdom)*, 2013, **54**, 4729–4761.
3 D. S. Sholl and R. P. Lively, *Nature*, 2016, **532**, 435–437.
4 E. Esposito, L. Dellamuzia, U. Moretti, A. Fuoco, L. Giorno and J. C. Jansen, *Energy Environ. Sci.*, 2019, **12**, 281–289.
5 M. Galizia, W. S. Chi, Z. P. Smith, T. C. Merkel, R. W. Baker and B. D. Freeman, *Macromolecules*, 2017, **50**, 7809–7843.
6 R. W. Baker and B. T. Low, *Macromolecules*, 2014, **47**, 6999–7013.
7 T. Masuda, E. Isobe, T. Higashimura and K. Takada, *J. Am. Chem. Soc.*, 1983, **105**, 7473–7474.
8 K. Nagai, T. Masuda, T. Nakagawa, B. D. Freeman and I. Pinnau, *Prog. Polym. Sci.*, 2001, **26**, 721–798.
9 Z. Cui, E. Drioli and Y. M. Lee, *Prog. Polym. Sci.*, 2014, **39**, 164–198.
10 I. Pinnau and L. G. Toy, *J. Memb. Sci.*, 1996, **109**, 125–133.
11 M. Yavari, M. Fang, H. Nguyen, T. C. Merkel, H. Lin and Y. Okamoto, *Macromolecules*, 2018, **51**, 2489–2497.
12 S. Kim and Y. M. Lee, *Prog. Polym. Sci.*, 2015, **43**, 1–32.
13 Z.-X. Low, P. M. Budd, N. B. McKeown and D. A. Patterson, *Chem. Rev.*, 2018, **118**, 5871–5911.
14 N. B. McKeown and P. M. Budd, *Macromolecules*, 2010, **43**, 5163–5176.
15 P. M. Budd, E. S. Elabas, B. S. Ghanem, S. Makhseed, N. B. McKeown, K. J. Msayib, C. E. Tattershall and D. Wang, *Adv. Mater.*, 2004, **16**, 456–459.
16 J. G. Wijmans and R. W. Baker, *J. Memb. Sci.*, 1995, **107**, 1–21.
17 J. G. Wijmans and R. W. Baker, *The Solution-Diffusion Model: A Unified Approach to Membrane Permeation*, 2006.
18 L. M. Robeson, *J. Memb. Sci.*, 1991, **62**, 165–185.
19 L. M. Robeson, *J. Memb. Sci.*, 2008, **320**, 390–400.
20 R. Swaidan, B. Ghanem and I. Pinnau, *ACS Macro Lett.*, 2015, **4**, 947–951.
21 B. Comesaña-Gándara, J. Chen, C. G. Bezzu, M. Carta, I. Rose, M.-C. Ferrari, E. Esposito, A. Fuoco, J. C. Jansen and N. B. McKeown, *Energy Environ. Sci.*, , DOI:10.1039/C9EE01384A.
22 B. D. Freeman, *Macromolecules*, 1999, **32**, 375–380.
23 C. R. Mason, L. Maynard-Atem, N. M. Al-Harbi, P. M. Budd,

P. Bernardo, F. Bazzarelli, G. Clarizia and J. C. Jansen, *Macromolecules*, 2011, **44**, 6471–6479.
24 I. Rose, C. G. Bezzu, M. Carta, B. Comesaña-Gándara, E. Lasseuguette, M. C. C. Ferrari, P. Bernardo, G. Clarizia, A. Fuoco, J. C. Jansen, K. E. E. Hart, T. P. Liyana-Arachchi, C. M. Colina and N. B. McKeown, *Nat. Mater.*, 2017, **16**, 932–937.
25 R. Williams, L. A. Burt, E. Esposito, J. C. Jansen, E. Tocci, C. Rizzuto, M. Lanč, M. Carta and N. B. McKeown, *J. Mater. Chem. A*, 2018, **6**, 5661–5667.
26 C. G. Bezzu, M. Carta, M.-C. Ferrari, J. C. Jansen, M. Monteleone, E. Esposito, A. Fuoco, K. Hart, T. P. Liyana-Arachchi, C. M. Colina and N. B. McKeown, *J. Mater. Chem. A*, 2018, **6**, 10507–10514.
27 A. Fuoco, R. M. Khdhayyer, P. M. Attfield, E. Esposito, C. J. Jansen and M. P. Budd, *Membr.* , 2017, 7.
28 H. Shamsipur, B. A. Dawood, P. M. Budd, P. Bernardo, G. Clarizia and J. C. Jansen, *Macromolecules*, 2014, **47**, 5595–5606.
29 S. Matteucci, Y. Yampolskii, B. D. Freeman and I. Pinnau, in *Materials Science of Membranes for Gas and Vapor Separation*, John Wiley & Sons, Ltd, 2006, pp. 1–47.
30 M. M. Dal-Cin, A. Kumar and L. Layton, *J. Memb. Sci.*, 2008, **323**, 299–308.
31 L. M. Robeson, B. D. Freeman, D. R. Paul and B. W. Rowe, *J. Memb. Sci.*, 2009, **341**, 178–185.
32 V. Teplyakov and P. Meares, *Gas Sep. Purif.*, 1990, **4**, 66–74.
33 D. W. Breck, *Zeolite molecular sieves: structure, chemistry, and use*, John Wiley & Sons, New York, N. Y., 1974.
34 L. M. Robeson, M. E. Dose, B. D. Freeman and D. R. Paul, *J. Memb. Sci.*, 2017, **525**, 18–24.
35 Y. Yampolskii, I. Pinnau and B. D. Freeman, *Materials Science of Membranes for Gas and Vapor Separation*, 2006.
36 P. Bernardo, J. C. Jansen, F. Bazzarelli, F. Tasselli, A. Fuoco, K. Friess, P. Izák, V. Jarmarová, M. Kačírková and G. Clarizia, *Sep. Purif. Technol.*, 2012, **97**, 73–82.
37 M. Macchione, J. C. Jansen, G. De Luca, E. Tocci, M. Longeri and E. Drioli, *Polymer (Guildf).*, 2007, **48**, 2619–2635.
38 J. C. Jansen and E. Drioli, *Polym. Sci. Ser. A*, 2009, **51**, 1355.
39 S. C. Fraga, M. Monteleone, M. Lanč, E. Esposito, A. Fuoco, L. Giorno, K. Pilnáček, K. Friess, M. Carta, N. B. McKeown, P. Izák, Z. Petrusová, J. G. Crespo, C. Brazinha and J. C. Jansen, *J. Memb. Sci.*, 2018, **561**, 39–58.
40 S. Li, J. L. Falconer, R. D. Noble and R. Krishna, *J. Phys. Chem. C*, 2007, **111**, 5075–5082.
41 Accelrys Software Inc, 2013.
42 H. Sun, *J. Phys. Chem. B*, 1998, **102**, 7338–7364.
43 W. J. Koros and C. Zhang, *Nat. Mater.*, 2017, **16**, 289.
44 A. Fuoco, B. Comesaña-Gándara, M. Longo, E. Esposito, M. Monteleone, I. Rose, C. G. Bezzu, M. Carta, N. B. McKeown and J. C. Jansen, *ACS Appl. Mater. Interfaces*, 2018, **10**, 36475–36482.
45 M. Carta, P. Bernardo, G. Clarizia, J. C. Jansen and N. B. McKeown, *Macromolecules*, 2014, **47**, 8320–8327.
46 P. M. Budd, N. B. McKeown, B. S. Ghanem, K. J. Msayib, D. Fritsch, L. Starannikova, N. Belov, O. Sanfirova, Y. Yampolskii and V. Shantarovich, *J. Memb. Sci.*, 2008, **325**, 851–860.
47 T. Masuda, Y. Iguchi, B. Z. Tang and T. Higashimura, *Polymer (Guildf).*, 1988, **29**, 2041–2049.
48 R. Smajda, Á. Kukovecz, Z. Kónya and I. Kiricsi, *Carbon N. Y.*, 2007, **45**, 1176–1184.
49 M. Kanezashi and Y. S. Lin, *J. Phys. Chem. C*, 2009, **113**, 3767–3774.
50 B. Jähne, G. Heinz and W. Dietrich, *J. Geophys. Res. Ocean.*, 1987, **92**, 10767–10776.
51 D. M. Himmelblau, *Chem. Rev.*, , DOI:10.1021/cr60231a002.
52 A. J. H. Boerboom and G. Kleyn, *J. Chem. Phys.*, 1969, **50**, 1086–1088.
53 E. Tocci, A. Gugliuzza, L. De Lorenzo, M. Macchione, G. De Luca and E. Drioli, *J. Memb. Sci.*, 2008, **323**, 316–327.
54 E. Tocci and P. Pullumbi, *Mol. Simul.*, 2006, **32**, 145–154.
55 J. C. Jansen, M. Macchione, E. Tocci, L. De Lorenzo, Y. P. Yampolskii, O. Sanfirova, V. P. Shantarovich, M. Heuchel, D. Hofmann and E. Drioli, *Macromolecules*, 2009, **42**, 7589–7604.
56 B. Satilmis, M. Lanč, A. Fuoco, C. Rizzuto, E. Tocci, P. Bernardo, G. Clarizia, E. Esposito, M. Monteleone, M. Dendisová, K. Friess, P. M. Budd and J. C. Jansen, *J. Memb. Sci.*, 2018, **555**, 483–496.
57 L. M. Robeson, Z. P. Smith, B. D. Freeman and D. R. Paul, *J. Memb. Sci.*, 2014, **453**, 71–83.
58 C. R. Mason, L. Maynard-Atem, K. W. J. Heard, B. Satilmis, P. M. Budd, K. Friess, M. Lanč, P. Bernardo, G. Clarizia and J. C. Jansen, *Macromolecules*, 2014, **47**, 1021–1029.